PHYSICAL REVIEW B VOLUME 47, NUMBER 4 15 JANUARY 1993-II

Carrier capture into a semiconductor quantum well

P. W. M. Blom, C. Smit, J. E. M. Haverkort, and J. H. Wolter
Department of Physics, Eindhoven University of Technology, P.O. Box 513, 5600 MB Eindhoven, The Netherlands
(Received 20 July 1992)

We experimentally observed an oscillating carrier capture time as a function of quantum well thickness. The capture times were obtained in a separate confinement quantum well structure by subpicosecond rise time measurements of the quantum well luminescence as well as by pump-probe correlation measurements of the population decay in the barrier layer. Both experimental techniques yield an oscillating capture time between 3 and 20 ps, in excellent agreement with the theoretical predictions. In a classical picture, our results correspond to a local capture time oscillating between 0.1 and 1.8 ps. Furthermore, the dependence of the capture time on the excitation energy is analyzed and the time-dependent position of the quasi-Fermi-level in the barrier layer is tracked experimentally. We find that the carrier capture time is very sensitive to the detailed structure parameters as well as to the carrier distribution in the barrier. Carrier capture is found to be an ambipolar process in which the oscillations of the observed capture times are due to the quantum-mechanical oscillation of the electron wave-function overlap above the well. Finally, electron capture is demonstrated to be dominated by LO-phonon emission.

I. INTRODUCTION

The capture of electrons and holes into semiconductor quantum well structures has received considerable interest in both fundamental and device-oriented research. For quantum well lasers, the capture efficiency is expected to influence both the quantum efficiency[1] and the dynamical performance.[2–4] In early theoretical studies,[5,6] the carrier capture was regarded as a classical process in which the carrier capture time defined a LO-phonon–scattering-limited mean free path in bulk GaAs. In these calculations, the bulk GaAs LO-phonon scattering time of 0.1 ps leads to a mean-free-path length of about 60 Å. As a result, carrier capture was expected to be efficient for quantum wells with thicknesses larger than 60 Å. In more recent studies,[7–10] the quantum-mechanical aspect of the capture process was taken into account. In this approach the capture time is expected to show resonances as a function of the quantum well thickness. The capture process, which is governed by the emission of LO phonons, is enhanced whenever a new bound state couples into the quantum well. For a $GaAs/Al_xGa_{1-x}As$ single-quantum-well (SQW) structure, capture times oscillating between 30 ps and 1 ns were predicted by Brum and Bastard.[8] Babiker and Ridley[9] reported capture times oscillating between 1–10 ps for a $GaAs/Al_xGa_{1-x}As$ superlattice, in which the formation of minibands and the folded spectrum of polar optical phonons was taken into account. Furthermore, they predicted[11] additional resonances in the carrier capture process in a superlattice due to the two-dimensional properties of the phonon states in the quantum wells of the superlattice. With respect to the carrier capture time, it is a major question whether the predicted oscillations in the carrier capture time exist or not. Or in other words, is the quantum-mechanical approach, which predicts these oscillations, correct or is the classical approach adequate?

Experimentally, most observed capture times seemed to contradict the theoretical predictions or at least did not show the predicted oscillations of the carrier capture time. Capture times of <20 ps,[12] 4 ps,[13] and 2–3 ps (Ref. 14) were obtained from time-resolved studies on SQW structures. From cw photoluminescence experiments on a $GaAs/Al_xGa_{1-x}As$ multiple-quantum-well (MQW) structure,[15] a capture time of 0.1 ps was derived. An electron capture time of <1 ps was reported[16,17] for $In_yGa_{1-y}As/InP$ MQW structures from time-resolved luminescence experiments and no well width dependence was observed. It was deduced that for thick barrier layers (>500 Å), the carrier capture process is dominated by drift and diffusion, while thin barrier layers (<200 Å) give rise to a quantum-mechanical process.

It was reported by Tsang[18] that the active layer thickness for MQW laser structures, which gives rise to an optimum laser performance, is of the order of 1000–1500 Å. The question whether the capture process in these laser structures is dominated by classical diffusion and drift (no oscillations expected) or by quantum-mechanical capture (oscillations expected) is relevant for the optimization of the capture efficiency in quantum well laser structures. In this paper, we have systematically studied the carrier capture process in four separate confinement heterostructure single-quantum-well structures (SCH SQW) with well widths of 30, 50, 70, and 90 Å. In the quantum-mechanical model,[8] the well widths of 30 and 70 Å correspond to a maximum in the capture time and the 50- and 90-Å quantum wells to a minimum. In the classical point of view, the quantum wells of 70 and 90 Å, which exceed the mean scattering length of 60 Å, are expected to collect the carriers more efficient than the 30- and 50-Å quantum wells.

 ©1993 The American Physical Society

The carrier capture times are experimentally studied by both the QW luminescence rise times (Sec. II A) and barrier luminescence decay measurements (Sec. II B). The dependence of the capture time on quantum well thickness (Sec. II C) and laser excess energy (Sec. II D) are reported. Furthermore, we tracked the Fermi level in the barrier during capture which will be reported in Sec. II E. In Sec. III A, we present a quantum-mechanical capture model which explains both the observed dependencies of the capture time on laser excess energy (Sec. III B) and quantum well thickness (Sec. III C). Finally, for device applications at high carrier densities, we deduce an oscillating local capture time (Sec. III D).

II. EXPERIMENTAL RESULTS

A. Rise time of the quantum well luminescence

The carrier capture process is studied in molecular-beam-epitaxy-grown $GaAs/Al_xGa_{1-x}As$ single-QW structures as shown in Fig. 1. These structures consist of ten separate single quantum wells, which are surrounded by 500-Å $Al_{0.33}Ga_{0.67}As$ barrier layers and 100-Å AlAs cladding layers. The capture times of photoexcited carriers in these SCH SQW structures is experimentally measured by two different techniques with picosecond resolution. In the first technique, we deduce the carrier capture times from subpicosecond time-resolved luminescence experiments using an up-conversion light-gate. It is based on a frequency mixing technique which was first introduced by Mahr and Hirsch.[19] In the up-conversion technique, the luminescence excited by an ultrashort laser pulse is mixed with the laser itself in a nonlinear crystal to generate the sum or difference frequency radiation. Since the mixing process takes place only during the presence of the laser pulse, this provides time-resolution comparable to the laser pulse width, provided certain conditions are satisfied.[20] Our laser system consists of a Coherent Antares mode-locked Nd:YAG (yttrium aluminum garnet) laser and a Coherent double jet synchronously pumped dye laser. The output of the laser system consists of a pulse train with a pulse width of 0.6 ps, a repetition rate of 76 MHz, and a typical output power of 200 mW. The capture times are determined from the differences in the rise time of the quantum-well luminescence after direct (below the barrier band gap) and indirect (above the barrier band gap) excitation with a subpicosecond laser pulse (0.6 ps). By comparing the QW luminescence rise times after the direct and indirect excitation, we eliminate the effect of relaxation of the carriers to the lowest level where the luminescence is detected. In order to obtain the same cooling inside the quantum well for direct and indirect excitation, the number of carriers inside the wells is kept constant in both experiments and the excitation energy for direct excitation is chosen as one LO-phonon energy (36 meV) times $(1+m_e^*/m_h^*)$ below the excitation energy for indirect excitation. The sample temperature was maintained at a temperature of 8 K in order to avoid phonon-absorption-induced heating of the carriers. In Fig. 2, the time evolution of the quantum well luminescence is shown for a 30-Å quantum well after direct and indirect excitation. This experiment was carried out at a laser intensity of 2 mW for indirect excitation, corresponding to a low excitation density of 3×10^{16} cm^{-3}. For indirect excitation, the laser excess energy with regard to the barrier band gap was 36 meV. By fitting the experimental rise times to simple rate equations,[21] we obtain a capture time of 19.1 ± 2 ps for this well width. Furthermore, no dependence of the capture time on the excitation density was found in the range 3×10^{15} to 2×10^{17} cm^{-3}. For larger excitation densities,

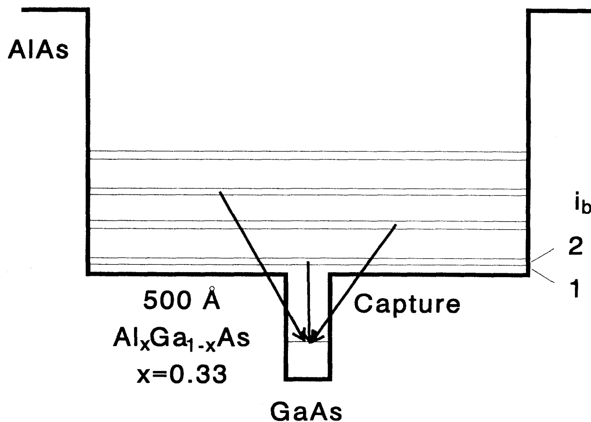

FIG. 1. A schematic of the carrier capture process in the $GaAs/Al_xGa_{1-x}As$ SCH single-QW structure considered in this study. The energy levels in the barrier (labeled $i_b=1.2,\ldots,$) appear in pairs with wave functions of even and odd symmetry with regard to the quantum well.

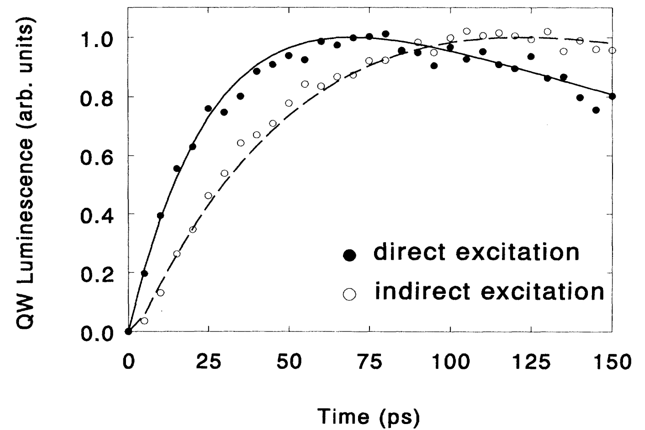

FIG. 2. Experimental determination of the carrier capture time using rise time differences of the quantum well luminescence after direct (closed circles) excitation into the quantum well and indirect (open circles) excitation into the $Al_xGa_{1-x}As$ barriers with a laser pulse (0.6 ps). The curves are fitted to the experiments using simple rate equations (Ref. 21). From these fits, a capture time of 20 ps is derived for this structure. The experiments were carried out at an excitation density of 2×10^{16} cm^{-3} and at a temperature of 8 K in a $GaAs/Al_xGa_{1-x}As$ SCH SQW structure with a well width of 30 Å.

no capture times could be obtained due to band filling in the quantum well.

B. Decay of the $Al_xGa_{1-x}As$ barrier luminescence

The rise time difference of the quantum well luminescence has been compared to the decrease of the carrier concentration of the barrier states. Therefore, we have performed two-pulse correlation experiments on the luminescence of the barrier states, a technique which was introduced by Mahar and Sagan.[22] In our experimental setup, we determine the absorption of the probe pulse by measuring the intensity of the time-integrated luminescence induced by the probe pulse as a function of the laser wavelength and of the pump-probe delay, yielding both the energy dependence and the temporal dependence of the carrier occupation. In a two-pulse correlation experiment, the photoluminescence (PL) *decay* of the barrier layers shows up as an *increase* of the correlated PL signal. This can be understood as follows: A strong excitation pulse (2×10^{17} cm^{-3}) creates electrons and holes in the barrier states and reduces the absorption of a second laser pulse (1×10^{17} cm^{-3}) with the same photon energy. If, however, the delay between the laser pulses exceeds the carrier capture time, then the absorption of the second laser pulse is no longer reduced. As a result, the barrier luminescence due to the probe pulse is expected to increase with increasing time delay between the laser pulses until the carriers of the first pulse are captured by the quantum well. In Fig. 3(a) the correlated barrier luminescence is shown for a 70-Å quantum well as a function of the delay between the laser pulses together with a fitted curve, which provides a capture time of 14.8 ± 2 ps. The temporal width of the laser pulses was 0.6 ps and the excess energy of the pump and probe pulse (2.014 eV) with regard to the barrier band gap (1.981 eV) was 33 meV. The detection energy (1.987 eV) was set to the maximum of the barrier luminescence with a broad detection window of 10 meV. The fact that the increase of the correlated barrier luminescence is actually due to an increase of the probe absorption is confirmed by a "transmission type" of experiment in which we detect the luminescence intensity of the bulk GaAs buffer layer, which is located between the substrate and the quantum wells. The intensity of the bulk GaAs luminescence peak decreases with decreasing probe *transmission* through the SCH QW structure, resulting in a decrease of this GaAs luminescence as a function of the pulse delay, as shown in Fig. 3(b). As expected, the time constant of the increase of the $Al_xGa_{1-x}As$ luminescence [Fig. 3(a)] is also found in the decrease of the GaAs luminescence [Fig. 3(b)] as a function of the delay between the laser pulses.

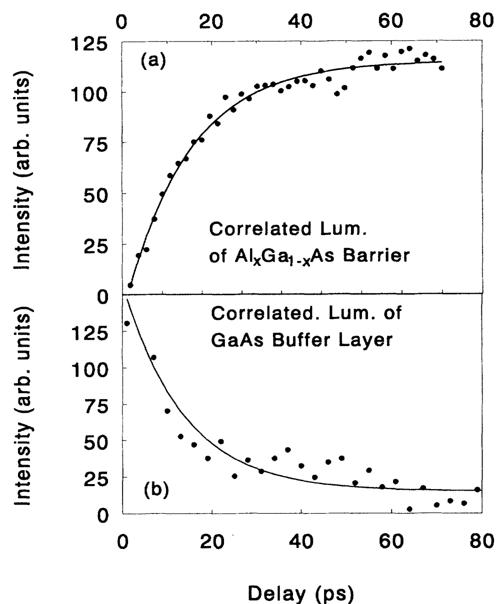

FIG. 3. Determination of the capture time from the decay of the barrier population. In the upper part, the correlated $Al_xGa_{1-x}As$ barrier luminescence is shown as a function of time delay between two laser pulses for a SCH QW with a 70-Å quantum well. The time increase of the probe-induced barrier luminescence results from a time increase of the absorption of the probe pulse and is directly related to the carrier capture time. In the lower part, the correlated luminescence of the GaAs buffer layer, which is located underneath the quantum wells, is plotted as function of the delay between the laser pulses. The decrease of the bulk GaAs luminescence arises from the fact that the transmission of the probe pulse through the quantum well structure decreases in time as a result of the carrier capture process.

C. Well width dependence of the carrier capture time

We have measured the capture time for a set of SCH QW samples with different quantum well thickness. The variation of the observed carrier capture times as a function of well width is shown in Fig. 4. In all measure-

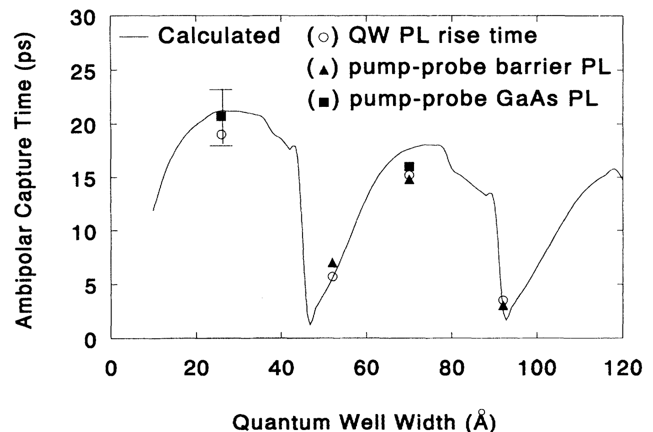

FIG. 4. Observation of an oscillating carrier capture time. The figure shows agreement between the experimentally observed capture times with the theoretical calculated ambipolar capture times. The experimental data have been obtained by (open circles) up-conversion measurement of the difference in QW rise times, by (closed triangles) two-pulse correlation measurements of the population decay in the barrier layers, and by (closed squares) "transmissionlike" correlation experiments detecting on the bulk GaAs PL signal.

ments, the excess energy of the laser with regard to the barrier band gap was located between 30–36 meV. We find oscillations in the carrier capture time between 3 and 20 ps as a function of quantum well width. It should be noted that for all samples the capture times obtained from the correlation measurements reproduce within experimental error (±2 ps) with the capture times derived from the quantum well rise times. Also included are the predictions of our ambipolar capture model. In this model, the variations of the capture time are governed by the quantum-mechanical electron capture time, as will be discussed in Sec. III. The observed capture times are in excellent agreement with the theoretically predicted ambipolar capture times.

The large discrepancies between predicted[8,9] (SQW and superlattice) and experimental[15,16] (MQW) capture times reported in literature and especially the lack of observed oscillations in the carrier capture time, were initially attributed[23] to the fact that the quantum-mechanical approach of the carrier capture process in quantum well structures would not be valid, because the barrier states are not coherent over the entire barrier width. For structures with thick barrier layers of 2000 Å, as regarded by those authors, the classical approach is expected to provide a more realistic description of the capture process than the quantum-mechanical model. However, in a recent theoretical study[24] we showed that the carrier capture efficiency in MQW structures not only oscillates as a function of well width but also as a function of the barrier width between the wells. This strong dependence of the carrier capture time on the quantum well and barrier width appears to be one of the main reasons for the large discrepancies between predicted and experimental capture times reported in the literature. The reported experimental results[15–17] for large MQW structures of <1 ps, which seem to contradict to the quantum-mechanical predictions[8] (SQW), are in very good agreement with the recent predictions of the quantum-mechanical capture times in precisely these large MQW structures.[24]

In order to verify the ambipolar character of the carrier capture, we measured the carrier capture times in samples with *p*- and *n*-doped quantum wells and undoped barrier layers. If the holes are captured first by the quantum well, the quantum well luminescence rise time of the *n*-doped sample should be faster than the rise time of the *p*-doped sample. In our experiments, no dependence of the carrier capture time on the dopant was observed, which confirms the ambipolar character of the carrier capture process. Because of the mutual agreement between the ambipolar capture model and two experimental methods for determining the structural dependence of the carrier capture time, we are confident that our ambipolar capture model provides a realistic description of the carrier capture process in SCH QW structures.

D. The carrier distribution in the barrier after excitation: Relevance for capture

We investigated the dependence of the carrier capture times on the population of the barrier subbands after excitation with a laser pulse. The carrier distribution function is dependent on the laser excess energy with regard to the barrier band gap. In Fig. 5, the observed rise of the correlated barrier luminescence is shown for laser excess energies of 32 and 36 meV in a SCH QW structure with a quantum well width of 50 Å. At a laser excess energy of 36 meV, as plotted in Fig. 6, we observe a sharp decrease of the carrier capture time from 20 to 6 ps. The 50-Å quantum well contains two bound states for the electrons, located at 190 and 4 meV below the barrier band gap, respectively. It should be noted that a laser ex-

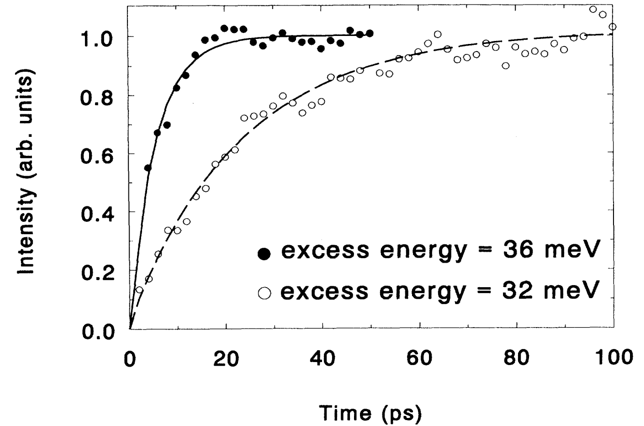

FIG. 5. Correlated $Al_xGa_{1-x}As$ barrier luminescence for a 50-Å SCH QW as a function of time delay between two laser pulses at laser excess energies of 32 meV (open circles) and 36 meV (closed circles) with regard to the barrier band gap. The fitted curves provide capture times of 22 and 6 ps for the excess energies of 32 meV (dashed line) and 36 meV (solid line), respectively. The experiments were carried out at an excitation density of 1×10^{17} cm^{-3} and a temperature of 8 K. The detection window was set to 10 meV.

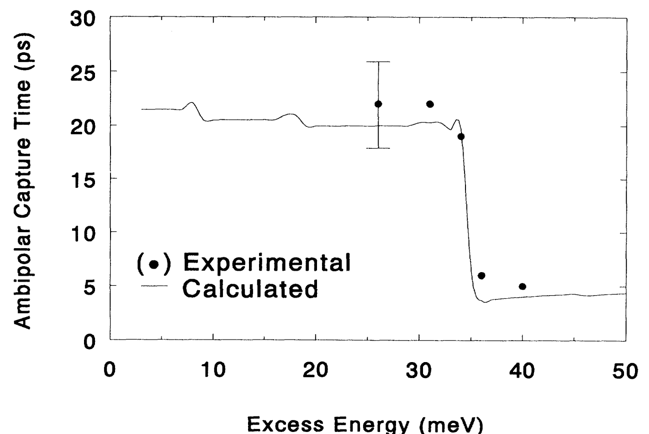

FIG. 6. Calculated (solid line) and experimental (closed circles) ambipolar capture time as a function of laser excess energy for a 50-Å quantum well structure. The observed decrease of the capture time at an excess energy of 36 meV originates from the presence of a quantum well bound state close (4 meV) to the continuum and proves that phonon emission is the dominant mechanism for capture.

cess energy of 36 meV with regard to the barrier band gap corresponds to an excess energy of 32 meV for the electrons and to an excess energy of only 4 meV for the heavy holes, due to the differences in the effective masses. Electrons with an excess energy larger than 32 meV are able to emit a 36-meV LO-phonon and are captured into the second subband, which is located only 4 meV below the barrier band gap. The electrons which have an excess energy of less than 32 meV with regard to the barrier band gap are only able to make a transition to the lowest bound state.

Furthermore, the sharp decrease of the carrier capture time demonstrates the dominance of the LO-phonon emission in the capture process as well as the quantum-mechanical character of the electron capture process. For the quantum wells with no bound state close to the continuum, only a slight decrease of the carrier capture time as a function of laser energy is observed. We did not measure the capture times for laser excess energies larger than 41 meV, since for these laser energies the electron excess energy exceeds 36 meV. As a result, the electrons are able to emit a LO phonon before the capture process which complicates the distribution function.

E. Measurement of the quasi-Fermi-level in the barrier

In the former experiments we showed that the carrier capture time depends on the population of the barrier states. The carrier capture time was determined by measuring the energy-integrated barrier luminescence with a broad detection wavelength window. For low carrier densities ($<2\times10^{17}$ cm^{-3}), where carrier-carrier scattering is small in comparison with LO-phonon emission, the carrier distribution in the barrier subbands after photoexcitation will be mainly determined by the capture times of the various subbands. At high-carrier densities ($>5\times10^{17}$ cm^{-3}), however, the photoexcited carriers will form a Fermi-Dirac-like distribution immediately after photoexcitation. In such an experiment, the number of carriers and thus the quasi-Fermi-level in the barrier layers will decrease, due to the capture process, as a function of time after excitation with a laser pulse. As a result, the population of the barrier subbands and thus the carrier capture time will be time dependent. Therefore, the carrier capture times, which are determined from the QW luminescence rise times and the barrier luminescence decay, are time-averaged values. We study the dynamical behavior of the carrier capture process by measuring the position of the quasi-Fermi-level after excitation with a subpicosecond laser pulse (0.6 ps) as a function of time. This can be achieved by reducing the detection wavelength window to 3 meV and then varying the *detection* energy at a fixed laser excess energy. After excitation with the first laser pulse (3×10^{17} cm^{-3}), the quasi-Fermi-level of the electrons in the barrier states starts to decrease due to the capture of the carriers. As long as the quasi-Fermi-level is above the detection energy, the carriers created by the weaker probe pulse (1×10^{17} cm^{-3}) will contribute to the luminescence at the detection energy and thus to the rise of the correlated barrier luminescence. If, however, the quasi-Fermi-level is below the detection energy, then the carriers of the second pulse will quickly relax down to the quasi-Fermi-level without contributing to the luminescence at the detection energy. As a result, the rise of the correlated barrier luminescence as a function of pulse delay stops at the moment the quasi-Fermi-level, which is determined by the number of carriers created with the pump pulse, has passed the detection energy. In our experiments, the quasi-Fermi-level is lifted with almost 9 meV by the second laser pulse, which means that the quasi-Fermi-level is 9 meV below our detection energy at the moment that the barrier luminescence reaches its maximum constant value. By measuring the rise time of the correlated barrier luminescence at various detection energies, we are able to track the electron quasi-Fermi-level as a function of time. In Fig. 7, the rise of the correlated barrier luminescence is shown for a 50-Å QW for detection energies located at 9 and 15 meV above the barrier band gap. The time constants of the correlated rise times are 25.0±2 and 15.2±2 ps, respectively. The excess energy of the laser with regard to the barrier band gap was 36 meV. By detecting at 15 meV above the barrier band gap we obtain from the rise time of 15.2 ps that the quasi-Fermi-level was located 6 meV above the barrier band gap 15 ps after excitation. In Fig. 8, the position of the observed quasi-Fermi-level with regard to the barrier band gap, which is determined from measurements at several detection energies, is plotted as a function of time. As stated above, the decrease of the carrier concentration and thus the quasi-Fermi-level after photoexcitation will be governed by a time-dependent capture time. The carrier capture process, however, is generally characterized by a time-averaged constant capture time. The calculat-

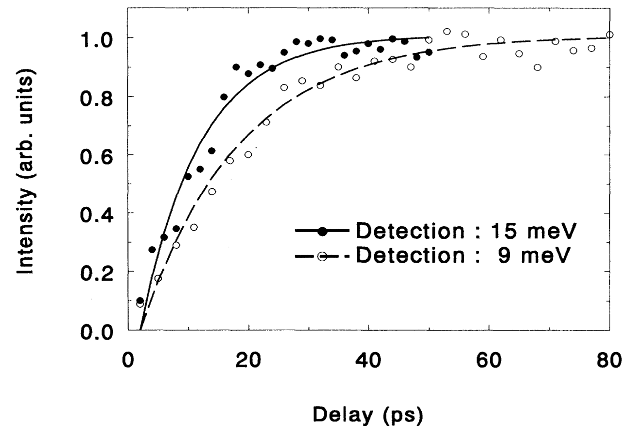

FIG. 7. Correlated $Al_xGa_{1-x}As$ barrier luminescence for a 50-Å SCH QW as a function of time delay between two laser pulses at detection energies of 9 (open circles) and 15 meV (closed circles) above the barrier band gap. The fitted curves provide capture times of 15 and 25 ps for the detection excess energies of 9 meV (dashed line) and 15 meV (solid line), respectively. The experiments were carried out with a laser excess energy of 36 meV at an excitation density of 2×10^{17} cm^{-3} and a temperature of 8 K. The detection window was set to 3 meV, which is the main difference with Fig. 5.

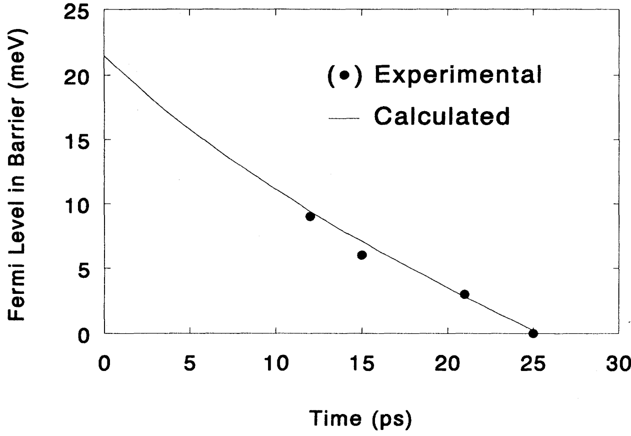

FIG. 8. Predicted (solid line) and measured (closed circles) position of the electron Fermi level in the barrier as a function of time after excitation with a laser pulse. The excess energy of the detection energies with regard to the barrier band gap was varied between 9–18 meV, whereas the laser excess energy of both the pump and probe pulse was constant at 36 meV.

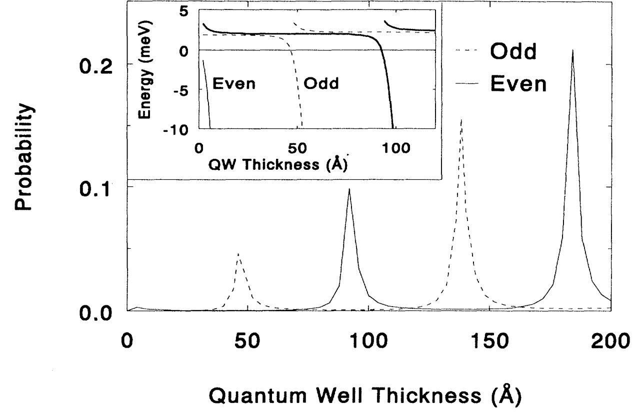

FIG. 9. The probability that an electron, which is energetically located in the lowest barrier state of the $Al_xGa_{1-x}As$ barriers, is spatially localized inside the GaAs quantum well layer as a function of the quantum well width for the structure shown in Fig. 1. The inset shows the position of the lowest two electron energy levels in the barrier with regard to the barrier band gap (0 meV). The probability peaks at those QW thicknesses where a new energy level is bound into the quantum well.

ed decrease of the quasi-Fermi-level due to the measured time-averaged capture time is also shown in Fig. 8 as the full curve. The agreement between the experimental points and the curve calculated with a time-averaged capture time suggests that the time-averaged capture time provides an adequate approximation of the dynamics of the capture process.

III. THEORY AND DISCUSSION

A. Quantum-mechanical calculation of the capture time

We consider a $GaAs/Al_xGa_{1-x}As$ SCH QW as shown in Fig. 1. The transition probability $W_{k,k'}$ for a carrier in an initial barrier state with wave vector k to emit a LO phonon and to become captured into a bound state in the quantum well with wave vector k' is given by[25]

$$W_{k,k'}=\frac{2\pi}{\hbar}\frac{1}{(2\pi)^3}\left|\int dq_z |I(q_z)|^2 |c|^2 \delta(k-k'-q)\right|_{xy} \times\delta[E_i(k)-E_f(k')-\hbar\omega] , \quad (1)$$

with q_z the phonon wave vector parallel to the growth axis, $I(q_z)$ the overlap integral between the quantum well and the barrier envelope functions

$$I(q_z)=\int dz \exp(-iq_z z)\psi_f^*(k')\psi_i(k) , \quad (2)$$

and $|c|$ the Fröhlich coupling constant for LO phonons,

$$|c|^2=\frac{1}{4\pi\epsilon_0}\frac{2\pi e^2\hbar\omega}{q^2}\left[\frac{1}{\epsilon_{r0}}-\frac{1}{\epsilon_{r\infty}}\right] . \quad (3)$$

The total scattering rate for a transition from an initial state to the allowed final states is given by

$$\tau(k)^{-1}=\int W_{k,k'}dk' . \quad (4)$$

First, we consider the envelope functions of the initial barrier states. The probability that an electron in a barrier state is located in the GaAs layer ("above" the well) is shown in Fig. 9 as a function of well width for the two lowest barrier states. It is shown that this probability is strongly enhanced for certain resonant well widths. In Fig. 10, the barrier wave function is plotted for a resonant quantum well width of 46 Å. We demonstrate that for the resonant well widths the wavelength of the barrier wave function above the quantum well exactly matches with the quantum well thickness. As a result, the wave function reaches its maximum value at the edge of the quantum well, which gives rise to a large probability of the electron being in the GaAs layer. These resonant wave functions appear at those quantum well widths where a barrier energy level is decreasing in energy and just starts to become a bound state by the quantum well.

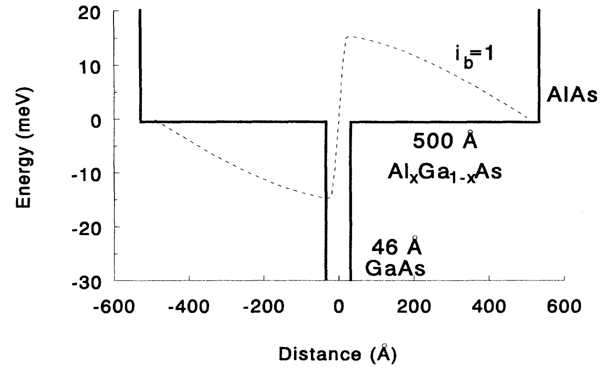

FIG. 10. The wave function (dashed line) of the lowest $Al_xGa_{1-x}As$ barrier state at a resonant quantum well width of 46 Å (see Fig. 9) as a function of the position parallel to the growth axis.

They correspond to the so-called virtual bound levels[8] and give rise to maxima in the overlap integral and thus to large capture rates for these well widths, since the final bound states are also localized in the GaAs layer.

The overlap integral [Eq. (2)], which contains the quantum well design by means of the wave functions, provides information about the relative strength of the LO-phonon-induced transitions between the different energy levels. In Fig. 11, the overlap integral is shown as a function of q_z for a transition of an electron in the lowest barrier state to the bound state of a 30-Å quantum well. The overlap integral vanishes at $q_z=0$ due to the orthogonality of the wave functions involved in the capture process. Furthermore, the overlap integral can be separated into a contribution of the overlap integral in the GaAs quantum-well layer and a contribution due to transitions in the $Al_xGa_{1-x}As$ barrier layers. The relative contribution of the transition in the GaAs layer is also plotted in Fig. 11. We demonstrate that the relative contribution due to transitions in the barrier layers to the overlap integral is twice as strong as the contribution of the quantum well layer in the overlap integral. This unexpected result is due to the fact that the wave function of the electron barrier state is located for 96% in the barrier layers and for only 4% in the quantum well layer, whereas the wave function of the bound state is located for 90% in the quantum well and for 10% in the barrier layers. Therefore, the overlap in the barrier layers of the wave functions involved in the capture process is larger than in the quantum well layer. As a result of the large contribution of the bulklike barrier layers to the capture process, we expect that the carrier capture process is well described by assuming bulk phonons. The incorporation of two-dimensional (2D) phonons[11] would only affect the contribution of the quantum well layers, which only dominates the capture process in structures with thin barrier layers such as, for example, superlattices.

B. Dependence on the barrier subband population

In Fig. 12, the overlap integral is plotted for several capture processes each starting from different barrier states into the same bound state of the 30-Å quantum well. We show that the carrier capture probability increases with increasing barrier subband number due to an improved overlap of the corresponding wave functions. As a result, the carrier capture time depends strongly on the population of the barrier subbands.

By calculating the carrier capture time we assume that there are no LO phonons present before excitation, thus there is no thermally activated escape from the well. Calculations of the carrier capture times were first presented by Brum and Bastard.[8] They found strong oscillations as a function of well width. They assumed a constant carrier distribution in the barrier states up to 36 meV above the barrier band gap for both electrons and the holes. This distribution corresponds to the situation where carriers are injected at very high excess energies and cool down to below 36 meV by emitting LO phonons. Our experiments, however, are carried out at low excess energies for which such a constant hole distribution is unrealistic. We approximate the initial carrier distribution function in the barrier subbands by calculating the overlap of the envelope functions of the hole and electron barrier states, which determines the absorption strength. From this approximation, we obtain that the *number* of barrier subbands which are occupied after absorption of a laser pulse is equal for both electrons and holes. So in our model, the initial states of the capture process are determined by the number of allowed transitions after absorption of a laser pulse. After excitation, the relaxation of the carriers in the barrier subbands is governed by carrier-carrier scattering and not by LO-phonon emission, since the separation of the barrier subbands (4–8 meV) is less than the LO-phonon energy (36.8 meV). The

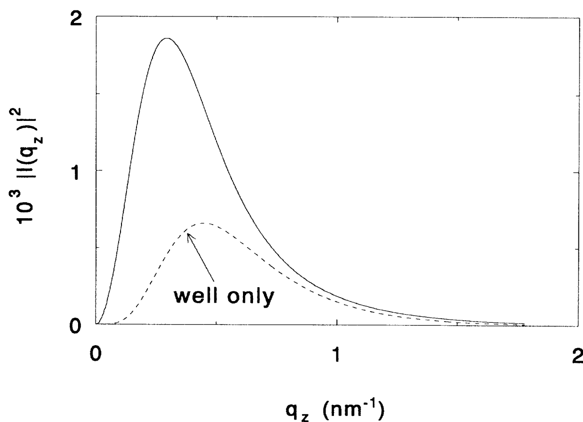

FIG. 11. The overlap integral $I(q_z)^2$ as a function of the phonon wave vector q_z (solid line) for a quantum well width of 30 Å. The relative contribution of the GaAs quantum well layer to the total overlap integral is shown as a dashed line.

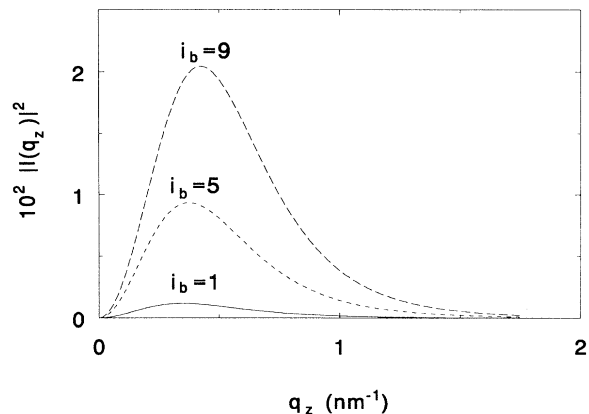

FIG. 12. The overlap integral $I(q_z)^2$ as a function of the phonon wave vector q_z for transitions from three barrier states to the bound state of a 30-Å quantum well. The overlap integral increases one order of magnitude between the lowest barrier state ($i_b=1$), which corresponds to the overlap integral of Fig. 11, and the ninth barrier state.

carrier-carrier scattering-induced intersubband transitions between the barrier states are relatively slow processes at carrier densities below 5×10^{17} cm^{-3}. The intersubband scattering is reduced by several orders of magnitude with regard to intrasubband scattering as a result of the orthogonality of the barrier wave functions involved in the scattering process.[26] Experimentally, a carrier-carrier-induced intersubband scattering time of 20 ps was observed[27] at a carrier density of 3×10^{17} cm^{-3}, which equals the density in our correlation experiments. Therefore, most of the carriers will only relax within a few hundred femtoseconds to their barrier subband minimum (intraband) during the capture process, resulting in an equal population of the barrier subbands. Our calculations show that the capture probability in a barrier subband is only slightly dependent on the exact position of the carrier in the subband. A difference in the carrier wave vector parallel in the quantum well plane only changes the length of the phonon vector in the capture process, not the overlap integral. Therefore, an increase of the excitation density from 2×10^{15} to 2×10^{17} cm^{-3} only affects the distribution of the carriers within each barrier subband and not the relative population of the different subbands. As a result, at these low excitation densities no large dependence of the carrier capture times on the excitation density is expected, which is consistent with our experimental observations.

We demonstrate in Fig. 13 for a 50-Å quantum well that the capture times of electrons and holes decrease whenever a new pair of barrier states is excited. The sharp decrease at an excess energy of 36 meV, which was also experimentally observed, originates from the presence of a quantum-well bound state located only 4 meV below the barrier band gap. Only electrons with an excess energy larger than 32 meV, which corresponds to a laser excess energy of 36 meV, are able to make a LO-phonon-induced transition to this bound state. The overlap of the wave function of this bound state with the wave functions of the barrier states and thus the capture rate is large, since the wave function of a bound state close to the continuum is only weakly confined in the quantum well layer. The electrons which have an excess energy of less than 32 meV with regard to the barrier band gap are only able to make a transition to the lowest bound subband. Such a transition results in a small capture rate due to the small overlap of the wave functions. The large phonon wave vectors involved in such a capture process also lead to a small capture rate, since the LO-phonon matrix element is inversely proportional to the square of the length of the phonon wave vector. We finally note that the carrier capture rate is limited by the relative slow capture rate of the electrons for small excess energies (<36 meV), whereas for high excess energies the capture rate is limited by the holes.

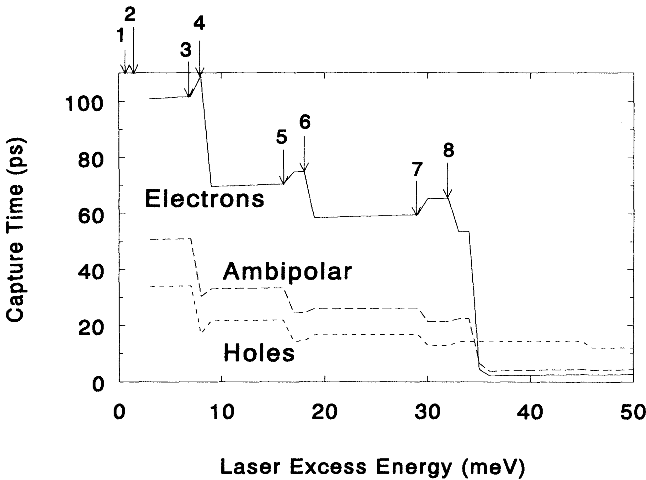

FIG. 13. Calculated electron, heavy hole, and ambipolar capture times as a function of the laser excess energy with respect to the barrier band gap, in a SCH QW structure with a well width of 50 Å. The positions of the energy levels in the barrier are indicated by the arrows. For excess energies larger than 36 meV the electrons are captured by the bound state which is only 4 meV below the continuum resulting in a sharp decrease of the capture time.

C. Ambipolar capture

At low excess energies, as in our experiments, holes will be captured by the well first and they will electrostatically attract electrons towards the quantum well, resulting in an increase of the electron capture rate. The remaining holes in the barrier layers will be electrostatically repelled by the well, which gives rise to a decrease of the hole capture rate. The net result is an ambipolar capture process with a capture rate which is in between the electron and hole capture rate. This ambipolar capture rate can be derived by inserting the electron and hole capture rates in a rate equation model. The solution of such a model reads as

$$\frac{dn_b}{dt}=-\frac{n_b}{\tau_e}-\frac{1}{2}\left[\frac{p_b}{\tau_h}-\frac{n_b}{\tau_e}\right]=-\frac{\tau_e+\tau_h}{2\tau_e\tau_h}n_b=-\frac{n_b}{\tau_a}\ , \tag{5}$$

$$\frac{dp_b}{dt}=-\frac{p_b}{\tau_h}+\frac{1}{2}\left[\frac{p_b}{\tau_h}-\frac{n_b}{\tau_e}\right]=-\frac{\tau_e+\tau_h}{2\tau_e\tau_h}p_b=-\frac{p_b}{\tau_a}\ , \tag{6}$$

with τ_e and τ_h the electron and hole capture times and τ_a the ambipolar capture time. The term $0.5^*(p_b/\tau_h-n_b/\tau_e)$ represents the increase and decrease of the electron and hole capture rate, respectively, as a result of their mutual electrostatic interaction.

The validity of the quantum-mechanical capture model for both electrons and holes is dependent on the coherence length of the carrier, which is limited by inelastic-scattering processes. For a coherence length which is small in comparison with the width of the barrier layers, the carriers are not able to establish coherent wave functions and the carriers should be regarded as a classical fluid. Quantization of the barrier states was observed[28] by photoluminescence excitation spectroscopy in $GaAs/Al_xGa_{1-x}As$ SCH SQW for structure widths up

to 750 Å. Furthermore, from a time-resolved luminescence study[29] on single quantum well structures with and without confinement layers an effective trapping area of about 800 Å was obtained. As a result, we expect that the carrier capture process in our structures, with a width of 1000 Å, is governed by the quantum-mechanical oscillations. It should be noted that the coherence length of the heavy holes is one order of magnitude smaller than the electron coherence length, due to a large effective mass which enhances the inelastic-scattering processes. As a result, the capture of the heavy holes should be described in terms of a classical diffusion process. Therefore, we expect that the ambipolar capture process in our structure is governed by a quantum-mechanical capture process of the electrons and a classical capture process of the holes. From steady-state photoluminescence experiments in GaAs/$Al_xGa_{1-x}As$ single quantum well structures, with a width of 1500 Å, resonances in the carrier capture were already observed as a function of well width.[30] Furthermore, it was demonstrated that the resonances were due to the quantum-mechanical character of the electron capture process, which supports our capture model. From the mobility of our n-doped bulk $Al_xGa_{1-x}As$ samples, we obtain a diffusion time of 12.5 ps for the holes in our structures. This classical diffusion time is also in agreement with the quantum-mechanical hole capture time for a laser excess energy of 36 meV, as shown in Fig. 13. As a result, we calculated our ambipolar capture time with a classical hole diffusion time, which is independent on well width, and a quantum-mechanical electron capture time, which shows oscillations as a function of well width. The well width dependence of our ambipolar capture time, as plotted in Fig. 4, is in excellent agreement with the experimental capture times. The predicted variations of the carrier capture time originate from the quantum-mechanical character of the electron capture process. The dependence of the capture time on the laser excess energy is very well described by the ambipolar capture model, as shown in Fig. 6 for the 50-Å quantum well. For the other samples only a slight decrease of the ambipolar carrier capture time with increasing the laser energy was predicted, which is in agreement with the experimental observations.

D. Local capture time

At very high carrier densities (1×10^{19} cm^{-3}), which are obtained in, for example, quantum-well laser amplifiers, the coherence length of the carriers is strongly reduced by carrier-carrier scattering. As a result, both the electrons and holes can be regarded as a classical fluid. In such a classical description a total classical diffusion model is used in combination with a local capture time, which purely characterizes the scattering process between the three-dimensional barrier states, which are spatially located in the well but energetically above the well, and the two-dimensional subbands for carriers which are spatially and energetically located in the quantum well. In order to obtain this local capture time we compare our quantum-mechanical model with the classical diffusion model. In the quantum-mechanical model the temporal dependence of the carrier density in the barrier layers, after excitation with a short laser pulse, is given by

$$n_b(t)=n_b(0)\exp(-t/\tau_a)\ , \tag{7}$$

with τ_a the ambipolar overall capture time. In the classical model this carrier density is described, neglecting recombination losses in the barrier, by a one-dimensional rate equation,

$$\frac{\delta n_b(z,t)}{\delta t}=D\frac{\delta^2 n_b(z,t)}{\delta z^2}-\frac{n_b(z,t)}{\tau_{\rm loc}}W\ , \tag{8}$$

with z the direction perpendicular to the quantum well layer. In this equation, D is the ambipolar diffusion constant, W is unity in the well and zero elsewhere, and $\tau_{\rm los}$ is the local capture time. This local capture time can be used as a fit parameter in order to equate the total carrier density in the barrier, resulting from Eq. (8), to the carrier density as given by Eq. (7) for a certain overall capture time as a function of time. Then the overall capture time is transferred into a local capture time and a diffusion constant.

The observed resonances of the overall capture time (3–20 ps) as a function of well width give rise to oscillations in the local capture time of 0.1–1.8 ps for a diffusion constant of 25 cm^2/s, as shown in Fig. 14. The increase of the amplitude of the oscillation with increasing well width is due to the fact that in the classical model the carrier capture rate is proportional to the well width. As a result, for a large well width, a relatively slow local capture time is needed to obtain a large flow of carriers into the quantum well. Therefore, the well width dependence of the carrier capture rate is obtained by normalizing the local carrier capture times to the quantum

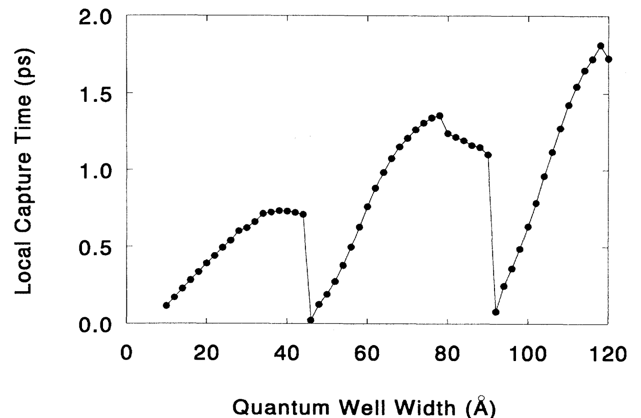

FIG. 14. Classically defined local electron capture time reduced from experiment as a function of quantum well thickness for a SCH single-QW structure. The ambipolar diffusion constant in the calculation was taken to be 25 cm^2/s, a value which is common for $Al_xGa_{1-x}As$.

well width. In our opinion a local capture time, which is dependent on well width, gives a more realistic description of the capture process in MQW laser structures at high carrier densities than the bulk GaAs LO-phonon scattering time of 0.1 ps.

Finally, we want to remark that the relatively small local capture time (0.1 – 1.8 ps), as well as its oscillations, are not insignificant for device performance. Although it may look like such a small local capture time can easily be neglected, it corresponds to quite large oscillations of the overall capture time (3 – 20 ps).

IV. CONCLUSIONS

In conclusion, we perform an experimental and theoretical study of the carrier capture time in $GaAs/Al_xGa_{1-x}As$ SCH QW structures. From both subpicosecond QW rise time, measurements and pump-probe correlation experiments on the barrier luminescence oscillations in the capture time between 3 and 20 ps were deduced as a function of quantum-well thickness. The observed capture times are in agreement with the theoretical predictions of an ambipolar capture model. In this model, the variations of the carrier capture times are due to the quantum-mechanical capture process of the electrons. The ambipolar character of the capture process was confirmed by experiments on doped samples. The dynamics of the capture process is studied by measuring the position of the quasi-Fermi-level as a function of time. From the dependence of the carrier capture time on the laser excess energy, we find that the capture times are very sensitive to the population of the barrier subbands. Furthermore, these experiments also reveal the dominance of the LO-phonon emission in the capture process. Finally, from a classical diffusion model we obtain that the observed capture times correspond to an oscillating local capture time in the range 0.1 – 1.8 ps.

ACKNOWLEDGMENTS

We would like to thank M. R. Leys and W. C. van der Vleuten for the growth of the quantum-well structures. This work is part of the research program of the Dutch Foundation for Fundamental Research on Matter (FOM), which is financially supported by the Dutch Organization for the Advancement of Research (NWO).

[1] P. W. M. Blom, P. J. van Hall, J. E. M. Haverkort, and J. H. Wolter, Proc. SPIE **1677**, 130 (1992).
[2] R. Nagarajan, T. Fukushima, S. W. Corzine, and J. E. Bowers, Appl. Phys. Lett. **59**, 1835 (1991).
[3] W. Rideout, W. F. Sharfin, E. S. Koteles, M. O. Vassell, and B. Elman, IEEE Photon. Technol. Lett. **3**, 784 (1991).
[4] S. D. Offsey, L. F. Lester, W. J. Schaff, and L. F. Eastman, Appl. Phys. Lett. **58**, 2336 (1991).
[5] H. Shichijo, R. M. Kolbas, N. Holonyak, Jr., J. J. Coleman, and P. D. Dapkus, Solid State Commun. **27**, 1029 (1978).
[6] J. Y. Tang, K. Hess, N. Holonyak, Jr., J. J. Coleman, and P. D. Dapkus, J. Appl. Phys. **53**, 6043 (1982).
[7] S. V. Kozyrev and A. Ya. Shik, Fiz. Tekh. Poluprovodn. **19**, 1667 (1985) [Sov. Phys. Semicond. **19**, 1024 (1985)].
[8] J. A. Brum, and G. Bastard, Phys. Rev. B **33**, 1420 (1986).
[9] M. Babiker and B. K. Ridley, Superlatt. Microstruct. **2**, 287 (1986).
[10] Y. Murayama, Phys. Rev. B **34**, 2500 (1986).
[11] M. Babiker, M. P. Chamberlain, A. Ghosal, and B. K. Ridley, Surf. Sci. **196**, 422 (1988).
[12] J. Feldmann, G. Peter, E. O. Göbel, K. Leo, H.-J. Polland, K. Ploog, K. Fujiwara, and T. Nakayama, Appl. Phys. Lett. **51**, 226 (1987).
[13] D. J. Westland, D. Mihailovic, J. F. Ryan, and M. D. Scott, Appl. Phys. Lett. **51**, 590 (1987).
[14] B. Deveaud, F. Clerot, A. Regreny, K. Fujiwara, K. Mitsunaga, and J. Ohta, Appl. Phys. Lett. **55**, 2646 (1989).
[15] D. Bimberg, J. Christen, A. Steckenborn, G. Weimann, and W. Schlapp, J. Lumin. **30**, 562 (1985).
[16] B. Deveaud, J. Shah, T. C. Damen, and W. T. Tsang, Appl. Phys. Lett. **52**, 1886 (1988).
[17] R. Kersting, X. Q. Zhou, K. Wolter, D. Grützmacher, and H. Kurz, Supperlatt. Microstruct. **7**, 345 (1990).
[18] W. T. Tsang, Appl. Phys. Lett. **38**, 204 (1980).
[19] H. Mahr and M. D. Hirsch, Opt. Commun. **13**, 96 (1975).
[20] J. Shah, IEEE J. Quantum Electron. **QE-24**, 276 (1988).
[21] E. O. Göbel, H. Jung, J. Kuhl, and K. Ploog, Phys. Rev. Lett. **51**, 1588 (1983).
[22] H. Mahar and A. G. Sagan, Opt. Commun. **39**, 269 (1981).
[23] A. Weller, P. Thomas, J. Feldmann, G. Peter, and E. O. Göbel, Appl. Phys. **A48**, 509 (1989).
[24] P. W. M. Blom, J. E. M. Haverkort, and J. H. Wolter, Appl. Phys. Lett. **58**, 2767 (1991).
[25] P. J. Price, Ann. Phys. (N.Y.) **133**, 217 (1981).
[26] S. M. Goodnick, and P. Lugli, Phys. Rev. B **37**, 2578 (1989).
[27] J. A. Levenson, D. Dolique, J. L. Oudar, and I. Abram, Phys. Rev. B **41**, 3688 (1990).
[28] M. H. Meynadier, C. Delalande, G. Bastard, M. Voos, F. Alexandre, and J. L. Liévin, Phys. Rev. B **31**, 5539 (1985).
[29] H.-J. Polland, K. Leo, K. Rother, K. Ploog, J. Feldmann, G. Peter, E. O. Göbel, K. Fujiwara, T. Nakayama, and Y. Ohta, Phys. Rev. B **38**, 7635 (1988).
[30] A. Fujiwara, S. Fukatsu, Y. Shiraki, and R. Ito, Surf. Sci. **263**, 642 (1992).